Macromolecular Theory and Simulations
www.mts-journal.de

Acrylate Network Formation by Free-Radical Polymerization Modeled Using Random Graphs

Verena Schamboeck, Ivan Kryven, and Pieter D. Iedema*

A novel technique is developed to predict the evolving topology of a diacrylate polymer network under photocuring conditions, covering the low-viscous initial state to full transition into polymer gel. The model is based on a new graph theoretical concept being introduced in the framework of population balance equations (PBEs) for monomer states (mPBEs). A trivariate degree distribution that describes the topology of the network locally is obtained from the mPBE, which serves as an input for a directional random graph model. Thus, access is granted to global properties of the acrylate network which include molecular size distribution, distributions of molecules with a specific number of crosslinks/radicals, gelation time/conversion, and gel/sol weight fraction. Furthermore, an analytic criterion for gelation is derived. This criterion connects weight fractions of converted monomers and the transition into the gel regime. Valid results in both sol and gel regimes are obtained by the new model, which is confirmed by a comparison with a "classical" macromolecular PBE model. The model predicts full transition of polymer into gel at very low vinyl conversion (<2%). Typically, this low-conversion network is very sparse, as becomes apparent from the predicted crosslink distribution.

1. Introduction

Inspired by recent developments concerning 3D printing and large-scale prints, inks based on mixes of multifunctional acrylates have become more and more attractive. Photocurable acrylate resins provide the possibility to create 3D objects by applying thin films of ink on a medium repeatedly. As the structure of cured acrylates has a strong impact on the final properties of the material, it is necessary to have an in-depth understanding of the formed networks. We present a novel mathematical model that gives insight into the topology of the network emerging during polymerization. This model is expected to greatly contribute to the improvement of material properties and optimization of process conditions in an efficient way.

V. Schamboeck, Dr. I. Kryven, Prof. P. D. Iedema
Van't Hoff Institute for Molecular Sciences
University of Amsterdam
P.O. Box 94157, 1090 GD Amsterdam, The Netherlands
E-mail: v.schamboeck@uva.nl

The ORCID identification number(s) for the author(s) of this article can be found under https://doi.org/10.1002/mats.201700047.

© 2017 The Authors. Published by WILEY-VCH Verlag GmbH & Co. KGaA, Weinheim. This is an open access article under the terms of the Creative Commons Attribution-NonCommercial License, which permits use, distribution and reproduction in any medium, provided the original work is properly cited and is not used for commercial purposes.

DOI: 10.1002/mats.201700047

This study focuses on the free-radical photo-polymerization of diacrylate monomers. During this process, two functional groups (vinyl groups) of each diacrylate monomer are converted into a maximum of four chemical bonds. Acrylate monomers with two or more functional groups have a dramatically different behavior than monoacrylates, since they form polymer networks rather than purely linear chains.[1] The structure of such a network plays a major role in defining the properties of the final material.[2,3] The infinite network is already seen to be formed[4] at remarkably low conversion of the multifunctional acrylates. This transition is called the gel point or percolation threshold.[5]

Several studies regarded the phase transition from sol to gel in multifunctional acrylate systems. In ref. [4], the conversion of vinyl groups was followed experimentally, while the gel point was observed by a microrheological method as a change in the system's rheology. Mathematical models describing the kinetics of acrylate polymerization appear in various studies.[6–17] Wen et al.[3] developed a model based on the cubic lattice percolation and confirmed the expectation that the kinetics is closely interlinked with the structure development of the polymer network due to radical trapping[18,19] and other reaction–diffusion phenomena.[20,21] Refs. [22–24] account for a termination rate that is dependent on the molecular size distribution. Most recently, a thiol–vinyl radical polymerization was investigated as a chemical alternative to acrylates.[25] The latter study predicts network structures that bear resemblance to those that appear in early modeling studies by Dušek.[26–28] Safranski and Gall[2] attempted to establish a link between thermomechanical properties of the photocuring system and the topology of the underlying network.

The methodology adopted in these studies can be viewed in a broader perspective of modeling for branched/crosslinked polymers. This field was initiated by Flory[5] based on analytical combinatorics and reaction kinetics. The combinatorial theory was then expanded by Stockmayer,[29] Ziff,[30] and others,[22,23,31,32] and culminated in the works by Dušek and Dušková-Smrčková, who combined both analytical methods and Monte Carlo (MC) simulations.[33] Notoriously, the analytical models are hard to custom-tailor to the specifics of the real-world chemical systems since the latter typically feature a mixture of monomers with functional groups of various kinds and substitution effects. This inability on one hand and increasingly

© 2017 The Authors. Published by WILEY-VCH Verlag GmbH & Co. KGaA, Weinheim

accessible computational power on the other resulted in a gradual shift of the focus to MC simulations,[34,35] population balance equation (PBE),[36–41] lattice modeling,[42] and molecular dynamics,[43] methodologies offering more flexibility than analytical models. Leiza and co-workers[44,45] were working on elaborate MC simulations for crosslink polymerization. Galina and Lechowicz[42] developed an MC method for 2D and 3D lattice networks based on the nearest-neighbor percolation process.

Despite increasing demand for PBE models in polymer reaction engineering, only a few chemical systems have a known analytical solution,[46] and in the most of these cases one has to apply an approximation technique. Many 1D and 2D PBEs were solved numerically by being transformed into partial differential equations in the generating function domain; see, for example, refs. [40,47]. The recent developments in approximation with radial basis functions gave access to modeling with multidimensional PBEs.[48] That said, solving PBEs numerically has an apparent drawback related to the "curse of dimensionality": the computational cost increases exponentially with an increasing number of dimensions.[49] Moreover, PBEs do not give direct access to samples of topology, while such samples are obtainable with MC simulations.

In this paper, we propose a model for radical acrylate photopolymerization that benefits from the synergy of three different modeling styles: analytical combinatorics, MC simulations, and PBEs. This approach is most accurately placed within the emerging field of "random graph modeling" that only recently started to diffuse into chemistry.[50–54] A random graph refers to a probability distribution over all possible realizations of a graph and allows us to draw results that are typical to MC simulations with an analytical probabilistic consideration. One of the most attractive features is that results on random graphs are often obtainable as an explicit exact equation bypassing any simulations at all.[52] Thus, the topology becomes accessible without the need of balancing expensive computational time against statistical errors.

In the current work, it is assumed that cycles only form in the gel. Models that do allow for cycles before gel were developed by Dušek and Dušková-Smrčková[55] in the context of PBEs and Eichinger[50] for random graphs.

The rest of the paper is organized as follows. Section 2 introduces the multifunctional acrylate photocuring problem formulated as a classical macromolecular PBE problem. Section 3 focuses on the local properties of the network. In this part, we introduce a monomer PBE (mPBE) that transit between various states. Similarly to the usual distinction between free monomers and monomers incorporated into polymer, we distinguish several extra categories: free monomer, monomer connected to the network with one bond, monomer connected with two bonds, etc. Additionally, these monomer states are differentiated by the type of bonds and the number of radicals/vinyl groups on a monomer. Throughout the rest of the paper, we write polymer PBE (pPBE) when referring to classical macromolecular PBE models (for example, as in ref. [48]) and mPBE when referring to the new monomer state balance. The mPBE model provides local topological information on the polymer network, in particular, the probability for a monomer to have a given number of specific bonds, which shapes as a trivariate "degree distribution." In Section 4, the local information provided by the degree distribution is used to construct the topology of the polymer network using random graph theory. To do so, we extend the ideas presented in refs. [52,56] to networks defined by a trivariate degree distribution. Utilizing this new formalism, global properties of the polymer network are obtained and analyzed. These include gelation time, gel/sol weight fraction, molecular size distribution, and other distributional properties of the acrylate network. Finally, the new approach is compared to a pPBE model from ref. [48] for validation.

2. Reaction Mechanism and pPBE

Like all radical polymerizations, photo-polymerization is based on three basic processes: initiation, propagation, and termination. In this paragraph, we follow the usual high-molecular formulation of radical polymerization. The state of a polymer $P_{s,v,r}$ is characterized by its size s, its number of vinyl groups v, also referred to as free pending double bonds (FPDBs), and radicals r.[9,57]

The chemical system, which is modeled in this paper, is based on the following reaction mechanism (see **Figure 1** for illustration):

- Photoinitiation (initiator I_2, initiator radical I)

$$I_2 \xrightarrow{k_d} 2I \tag{1}$$

- Initiation of a vinyl group (free divinyl monomer M_2)

$$I + M_2 \xrightarrow{2k_i} P_{1,1,1} \tag{2}$$

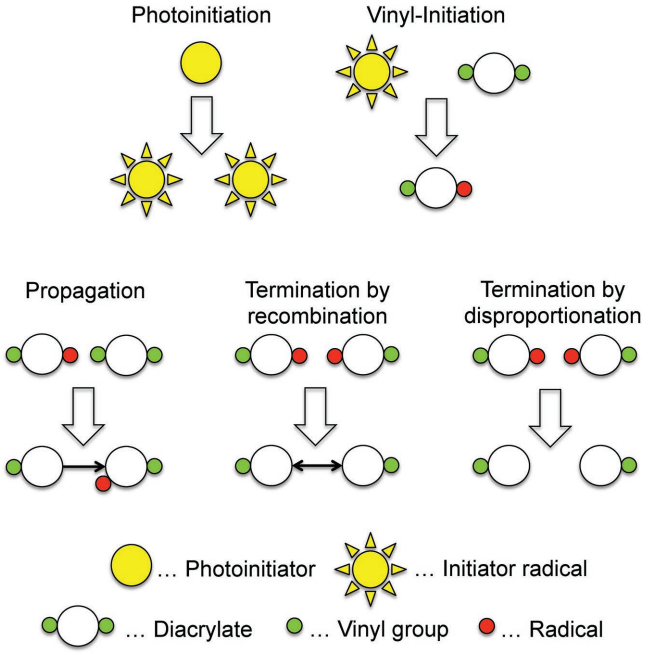

Figure 1. Illustration of the reaction mechanism. The directed bond connecting the monomer units in the "Propagation" column denotes an out-bond for the left unit and an in-bond for the right unit. Under "Termination by recombination," the units are connected by a bidirectional bond, which counts as a bidirectional bond for both units.

© 2017 The Authors. Published by WILEY-VCH Verlag GmbH & Co. KGaA, Weinheim

$$I + P_{s,\nu,r} \xrightarrow{\nu k_i} P_{s,\nu-1,r+1} \tag{3}$$

- Propagation

$$M_2 + P_{s,\nu,r} \xrightarrow{2rk_p} P_{s+1,\nu+1,r} \tag{4}$$

- Crosslinking

$$P_{s,\nu,r} + P_{s',\nu',r'} \xrightarrow{\nu r' k_p} P_{s+s',\nu+\nu'-1,r+r'} \tag{5}$$

- Termination by disproportionation

$$P_{s,\nu,r} + P_{s',\nu',r'} \xrightarrow{rr' k_{td}} P_{s,\nu,r-1} + P_{s',\nu',r'-1} \tag{6}$$

- Termination by recombination

$$P_{s,\nu,r} + P_{s',\nu',r'} \xrightarrow{\nu r' k_{tc}} P_{s+s',\nu+\nu',r+r'-2} \tag{7}$$

The parameters k_d, k_i, k_p, k_{td}, and k_{tc} represent the rate constants for each reaction with their numerical values listed in **Table 1**. In principle, during termination by disproportionation of acrylates, a terminal double bond is produced on one of the reacting monomer units. As this has little impact on the final topology, the terminal double bond is neglected in the present implementation of the reaction scheme.

The state of the chemical system is defined by the following pPBE

$$\begin{pmatrix} \dot{f}_{s,\nu,r} \\ [\dot{I}_2] \\ [\dot{I}] \\ [\dot{M}_2] \\ \dot{c}_r \\ \dot{c}_\nu \\ \dot{c}_c \end{pmatrix} = \begin{pmatrix} F_{s,\nu,r} \\ -k_d[I_2] \\ 2k_d[I_2] - k_i(2[M_2]+c_\nu)I \\ -2k_i[M_2][I] - 2k_p[M_2]c_r \\ k_i(2[M_2]+c_\nu)[I] - 2(k_{td}+k_{tc})c_r^2 \\ k_i(2[M_2]-c_\nu)[I] + 2k_p[M_2]c_r - k_p c_\nu c_r \\ k_p c_\nu c_r + k_i c_\nu I \end{pmatrix} \tag{8}$$

The left-hand side denotes the time derivative of several time-dependent functions. For reasons of readability the explicit time dependency of these functions is omitted. The

Table 1. Parameters defining the chemical system and the reaction mechanism are listed. This table includes the values of the initial concentration of divinyl monomers $[M_2](0)$ and initiator $[I_2](0)$, as well as the rate coefficients.[9]

Symbol	Value	Definition
$[M_2](0)$	4.75 mol L^{-1}	Initial concentration of the diacrylate
M_x	226 g mol^{-1}	Molar mass of the diacrylate
$[I_2](0)$	0.10 mol L^{-1}	Initial concentration of initiator
k_d	0.1296 s^{-1}	Rate coefficient of photoinitiation
k_i	6.1197×10^4 $(s\ mol)^{-1}$	Rate coefficient of vinyl initiation
k_p	6.1197×10^4 $(s\ mol)^{-1}$	Rate coefficient of propagation
k_{td}	4.3955×10^7 $(s\ mol)^{-1}$	Rate coefficient of termination by recombination
k_{tc}	4.3955×10^7 $(s\ mol)^{-1}$	Rate coefficient of termination by disproportionation

pPBE determining the molar concentration $f_{s,\nu,r} = [P_{s,\nu,r}]$ of a polymer state $\{s, \nu, r\}$ as a function of time t is characterized by

$$F_{s,\nu,r} = \phi_i + \phi_p + \phi_c + \phi_{td} + \phi_{tc} \tag{9}$$

with $F_{s,\nu,r}$ being defined as the right-hand side of the pPBE. Variable s denotes the size of the component; ν describes the number of FPDBs; and r defines the number of radicals of the component. The initiation rate of monomeric and polymeric vinyl groups ϕ_i is defined as

$$\phi_i = 2k_i[M_2][I]\delta_{s-1,\nu-1,r-1} + k_i[I]\left((\nu+1)f_{s,\nu+1,r-1} - \nu f_{s,\nu,r}\right) \tag{10}$$

where $\delta_{s,\nu,r}$ is defined as $\delta_{0,0,0} = 1$ and $\delta_{s,\nu,r} = 0$ for $s \neq 0$, $\nu \neq 0$, $r \neq 0$. The propagation rate ϕ_p is defined as

$$\phi_p = 2k_p r[M_2](f_{s-1,\nu-1,r} - f_{s,\nu,r}) \tag{11}$$

the crosslinking rate ϕ_c is given by

$$\phi_c = k_p \sum_{(s',\nu',r')=(1,0,1)}^{(s-1,\nu,r)} r'(\nu-\nu'+1) f_{s',\nu',r'} f_{s-s',\nu-\nu'+1,r-r'} - k_p(c_r\nu + c_\nu r) f_{s,\nu,r} \tag{12}$$

the termination rate by disproportionation ϕ_{td} is defined as

$$\phi_{td} = 2k_{td}c_r\left((r+1)f_{s,\nu,r+1} - r f_{s,\nu,r}\right) \tag{13}$$

and the termination rate by recombination ϕ_{tc} is given by

$$\phi_{tc} = k_{tc} \sum_{(s',\nu',r')=(1,0,1)}^{(s-1,\nu,r+1)} r'(r-r'+2) f_{s',\nu',r'} f_{s-s',\nu-\nu',r-r'+2} - 2k_{tc}c_r r f_{s,\nu,r} \tag{14}$$

The functions c_r, c_ν, and c_c denote the total molar concentration of radicals, FPDBs, and crosslinks; $[M_2]$ and $[I]$ correspond to the molar concentration of unreacted monomers and initiator radicals.

The function $f_{s,\nu,r}$ describes finite-sized molecules. Consequently, the gel, an infinite molecule, is not captured. The first moments of $f_{s,\nu,r}$ are defined as

$$\begin{aligned} c_{s,\mathrm{sol}} &= \sum_{s,\nu,r} s f_{s,\nu,r} \\ c_{c,\mathrm{sol}} &= \sum_{s,\nu,r} (s-\nu) f_{s,\nu,r} \\ c_{\nu,\mathrm{sol}} &= \sum_{s,\nu,r} \nu f_{s,\nu,r} \\ c_{r,\mathrm{sol}} &= \sum_{s,\nu,r} r f_{s,\nu,r} \end{aligned} \tag{15}$$

with the number of crosslinks of a molecule being defined by

$$c = s - \nu \tag{16}$$

Before the gel point, the moments $c_{s,\mathrm{sol}}$, $c_{c,\mathrm{sol}}$, $c_{\nu,\mathrm{sol}}$, and $c_{r,\mathrm{sol}}$ coincide with the total concentration of reacted monomer units c_s, crosslinks c_c, FPDBs c_ν, and radicals c_r. After the gel point, the total number of monomer units is not conserved for $f_{s,\nu,r}$ and its moments only apply to the sol part of the chemical system, which only includes finite-sized molecules. This implies that

© 2017 The Authors. Published by WILEY-VCH Verlag GmbH & Co. KGaA, Weinheim

the total concentration of crosslinks c_c, FPDBs c_v, and radicals c_r need to be modeled independently of $f_{s,\,v,\,r}$ and are therefore included in Equation (8). The derivations of the right-hand side expressions of Equation (8) that correspond to $\dot{c}_r$, $\dot{c}_v$, and $\dot{c}_c$ using Equation (9) and Equations (10)–(14) are available in the Supporting Information.

In principle, the three variables s, v, and r characterizing the polymer are unbounded. Especially s and v reach very high values during the polymerization process. For the numerical evaluation, an exact point-wise approach is not feasible as the pPBE would lead to a prohibitory number of differential equations: one for each combination of s, v, and r. A numerical recipe to solve the macromolecular polymerization problem was developed by Kryven and Iedema.[48] This method is used to solve the high-molecular formulation of our problem. Its results serve as a comparison to the new random graph model (RGM) in Section 5.1.

3. The mPBE

The essential idea of the random graph approach is to first solve the mPBE generating the connectivity of monomer units in the polymer and then recover the polymer properties, such as the gel point and the weight distribution of the polymers, by a combinatorial argument. In contrast to the well-established pPBE, focusing mainly on the size of the polymer, we calculate the concentration of the states of monomer units determining the number of bonds per monomer unit as a function of time and then construct global properties such as the molecular size distribution in the RGM.

A state of a diacrylate monomer unit (see Figure 1) is characterized by the number of vinyl groups v, radicals r, and the number of bonds, also referred to as the degree d, which is differentiated into three values: i, j, and k with $d = i + j + k$. The necessity of this differentiation arises from the different types of reactions. Later, when reconstructing the topology of the molecules, it is essential to ensure that two monomer units get connected by a bond only if both of them were subject of the same reaction (e.g., both underwent termination by recombination). Therefore, it is necessary to store information on the history of the bond formation. We distinguish bonds formed by the "asymmetrical" propagation reaction (radical reacts with vinyl group) and the "symmetrical" termination by recombination (radical reacts with radical). Let us define the direction of the propagation reaction from the radical toward the vinyl group (see Figure 1, "Propagation"). The monomer unit with a radical gets an out-bond, whereas the second monomer unit with the vinyl group gains an in-bond. Note that in the present work, the in-bond/out-bond notation has a different meaning than, for instance, in the work of Eichinger.[50] The bond formed by termination will be referred to as a "bidirectional" bond — as distinct from the asymmetrical bonds (see Figure 1, "Termination by recombination"). A monomer unit with an out-bond can only be connected to a monomer unit with an in-bond, whereas a monomer unit with a bidirectional bond connects to another monomer unit with a bidirectional bond. Information concerning the directionality is required if the degree distribution is not symmetric with respect to in- and out-bonds.[52] The monomer state is then defined by the number of in-bonds i, out-bonds j, and bidirectional bonds k, additionally to v and r.

Let $M_{v,\,r,\,i,\,j,\,k}$ be a monomer unit with its state being defined by the set of variables $\{v,\,r,\,i,\,j,\,k\}$ and $g_{v,\,r,\,i,\,j,\,k} = [M_{v,\,r,\,i,\,j,\,k}]$ be the concentration of the monomers in this state. As the five dimensions of $M_{v,\,r,\,i,\,j,\,k}$ are small (for diacrylates the possible values are $\{0, 1, 2\}$), solving the mPBE numerically is not hard.

The model is applied to photo-polymerization of a system consisting of diacrylates (two vinyl sites per monomer) and a photoinitiator. Similarly to Equations (1)–(7), we can now write the reaction mechanisms for monomer states $M_{v,\,r,\,i,\,j,\,k}$ (see Figure 1), which is defined as follows:

- Photoinitiation of the initiator

$$I_2 \xrightarrow{k_\mathrm{d}} 2I \tag{17}$$

- Initiation of a vinyl group

$$I + M_{v,r,i,j,k} \xrightarrow{vk_\mathrm{i}} M_{v-1,r+1,i,j,k} \tag{18}$$

- Propagation (also including crosslinking)

$$M_{v,r,i,j,k} + M_{v',r',i',j',k'} \xrightarrow{rv'k_\mathrm{p}} M_{v,r-1,i,j+1,k} + M_{v'-1,r'+1,i'+1,j',k'} \tag{19}$$

- Termination by disproportionation

$$M_{v,r,i,j,k} + M_{v',r',i',j',k'} \xrightarrow{rr'k_\mathrm{td}} M_{v,r-1,i,j,k} + M_{v',r'-1,i',j',k'} \tag{20}$$

- Termination by recombination

$$M_{v,r,i,j,k} + M_{v',r',i',j',k'} \xrightarrow{rr'k_\mathrm{tc}} M_{v,r-1,i,j,k+1} + M_{v',r'-1,i',j',k'+1} \tag{21}$$

In contrast to the definition of $P_{s,\,v,\,r}$, $M_{v,\,r,\,i,\,j,\,k}$ does include the state of unreacted (free) monomers, which corresponds to $M_{2,\,0,\,0,\,0,\,0}$. The reactions satisfy the conditions $0 \leqslant i, i', j, j', k, k' \leqslant 2$, $i + j + k \leqslant 4$, $i' + j' + k' \leqslant 4$, $j + k \leqslant 2$, and $j' + k' \leqslant 2$ intrinsically. Outside this range, $[M_{v,\,r,\,i,\,j,\,k}]$ is zero for all time. The reaction mechanism leads to 39 distinct states of a monomer unit that become populated in the course of the polymerization process.

The state of the chemical system is described by the mPBE, which is summarized to

$$\begin{pmatrix} \dot{g}_{v,r,i,j,k} \\ [\dot{I}_2] \\ [\dot{I}] \end{pmatrix} = \begin{pmatrix} G_{v,r,i,j,k} \\ -k_\mathrm{d}[I_2], \\ 2k_\mathrm{d}[I_2] - k_\mathrm{i}[I]c_v \end{pmatrix} \tag{22}$$

The left-hand side denotes the time derivatives of the concentrations of all monomer states $g_{v,\,r,\,i,\,j,\,k} = [M_{v,\,r,\,i,\,j,\,k}]$, as well as the initiator $[I_2]$ and initiator radicals $[I]$. The right-hand side of the mPBE determining the concentration of monomer states at time t reads

$$\begin{aligned} G_{v,r,i,j,k} = {} & k_\mathrm{i}[I]\left((v+1)g_{v+1,r-1,i,j,k} - vg_{v,r,i,j,k}\right) \\ & + k_\mathrm{p}c_r\left((v+1)g_{v+1,r-1,i-1,j,k} - vg_{v,r,i,j,k}\right) \\ & + k_\mathrm{p}c'_v\left((r+1)g_{v,r+1,i,j-1,k} - rg_{v,r,i,j,k}\right) \\ & + 2k_\mathrm{td}c_r\left((r+1)g_{v,r+1,i,j,k} - rg_{v,r,i,j,k}\right) \\ & + 2k_\mathrm{tc}c_r\left((r+1)g_{v,r+1,i,j,k-1} - rg_{v,r,i,j,k}\right) \end{aligned} \tag{23}$$

© 2017 The Authors. Published by WILEY-VCH Verlag GmbH & Co. KGaA, Weinheim

The functions c_r and c'_ν correspond to the total concentration of radicals and vinyl groups in the system. It is important to note the difference between c'_ν and c_ν: c_ν only accounts for FPDBs, whereas c'_ν also includes vinyl groups of the unreacted monomer units $g_{2,0,0,0,0}$.

In contrast to the pPBE model, here, the total concentration of crosslinks c_c, reacted monomer units c_s, and FPDBs c_ν (sol + gel) coincide with the first moments of $g_{\nu,r,i,j,k}$ and are calculated by

$$\begin{aligned} c_r &= \sum_{\nu,r,i,j,k} r g_{\nu,r,i,j,k} \\ c'_\nu &= \sum_{\nu,r,i,j,k} \nu g_{\nu,r,i,j,k} \\ c_\nu &= c'_\nu - 2g_{2,0,0,0,0} \\ c_c &= \sum_{\nu,r,i,j,k} g_{\nu,r,i,j,k}\Theta(i+j+k-3) \\ c_s &= \sum_{\nu,r,i,j,k} g_{\nu,r,i,j,k} - g_{2,0,0,0,0} \end{aligned} \tag{24}$$

with the Heaviside function

$$\Theta(x) = \begin{cases} 1, & \text{for } x \geq 0 \\ 0, & \text{for } x < 0 \end{cases} \tag{25}$$

Note that the mPBE allows us to easily distinguish between linear sequences (monomer units with two bonds) and crosslinks (three or four bonds).

Solving the system of Equation (8) numerically gives the concentrations of monomer states $g_{\nu,r,i,j,k}$. Once the concentrations $g_{\nu,r,i,j,k}$ are known, the trivariate degree distribution $u(i, j, k)$ is extracted. The distribution $u(i, j, k)$ defines the probability of a monomer unit for having i in-, j out-, and k bidirectional bonds as a function of time t. The normalized trivariate degree distribution $u(i, j, k)$ is calculated by

$$u(i,j,k) = \frac{\sum_{\nu,r} g_{\nu,r,i,j,k}}{\sum_{\nu,r,i,j,k} g_{\nu,r,i,j,k}} \tag{26}$$

with

$$\sum_{i,j,k} u(i,j,k) = 1 \tag{27}$$

Let μ_{lmn} denote the partial moments of the degree distribution $u(i, j, k)$ with

$$\mu_{lmn} = \sum_{i,j,k} i^l j^m k^n u(i,j,k) \tag{28}$$

Since the number of in-bonds and out-bond is equal, $\mu_{100} = \mu_{010}$. This equality naturally evolves from the reaction scheme. Note that these moments must be distinguished from the moments of the molecular size distribution.

4. The Random Graph Model

The aim of the current section is the derivation of a method to capture global properties of the network using a random graph formalism. The method represents an extension to previous works for undirected[56] and directed graphs without bidirectional edges.[52]

We view a group of connected monomers, essentially a polymer molecule, as a directed graph. Let us start by introducing some basic terminology of graph theory. The chemical bonds between the monomer units are viewed as the edges of the graph, the monomer units are referred to as the nodes, and the number of bonds of a monomer unit is called the degree of the node. Therefore, we call $u(i, j, k)$ the degree distribution. A polymer is thus represented as connected nodes, also called a connected component. Hence, we will refer to the out-bonds as out-edges, to the in-bonds as in-edges, and to the bidirectional bonds as bidirectional edges. An out–in connection between two nodes is resembled by a directed edge, an arrow, with its direction being defined as pointing from the node with an out-edge (former radical site) to the node with an in-edge (former vinyl site). For a bidirectional connection between nodes, no starting and end points can be defined.

After the degree distribution is recovered from the mPBE, the global properties of the network are found by applying a random graph formalism. We will introduce a mathematical method utilizing generating functions to solve the global problem and recover some typical global characteristics like the gel point, the size of the giant component, and the molecular size distribution.

4.1. Generating Functions

Generating functions provide an elegant way of deriving global properties of the graph. Here, we follow a similar line of reasoning as in our previous paper discussing the bivariate (in- and out-bonds) variant of this problem.[52] First, the distribution $u(i, j, k)$ is transformed to its generating function

$$U(x,y,z) = \sum_{i,j,k} u(i,j,k) x^i y^j z^k \tag{29}$$

with $|x|, |y|, |z| \leqslant 1$ and $x, y, z \in \mathbb{C}$. In this section, all newly introduced variables denoted by a capital letter indicate generating functions. $U(x, y, z)$ satisfies

$$U(1,1,1) = \sum_{i,j,k} u(i,j,k) = 1 \tag{30}$$

which corresponds to the normalization of the total probability. The partial moments of the degree distribution are obtained as the partial derivatives of the generating function $U(x, y, z)$ and the evaluation at point $(x, y, z) = (1, 1, 1)$

$$\mu_{lmn} = \left[\left(x\frac{\partial}{\partial x} \right)^l \left(y\frac{\partial}{\partial y} \right)^m \left(z\frac{\partial}{\partial z} \right)^n U(x,y,z) \right] \Big|_{x=y=z=1} \tag{31}$$

For illustration purpose, let us consider the following example. The first moment of the in-edges, equivalent to the average number of in-edges of a node, is derived from the generating function of the degree distribution by

© 2017 The Authors. Published by WILEY-VCH Verlag GmbH & Co. KGaA, Weinheim

$$\mu_{100} = x\frac{\partial}{\partial x}U(x,y,z)|_{x=y=z=1} = \sum_{i,j,k} iu(i,j,k) \tag{32}$$

Another important property of generating functions involves the transformation of the convolution operation. In the domain of generating functions, a convolution of two distributions $(g*f)(i, j, k)$ simplifies to the point-wise multiplication of their generating functions $G(x, y, z)F(x, y, z)$.

4.2. Component Size Distribution

The directed network is described as locally tree like. For the formulation of the random graph, several distributions are employed from the initial degree distribution $u(i, j, k)$. If a node is sampled at random, its degree is given by $u(i, j, k)$ by definition. Let us select a node by following a randomly chosen edge in some arbitrary direction. We are interested in the probability of this node to be connected to further nodes, which can be formulated by introducing a bias in the original degree distribution. For a node reached by an in-edge, the biased degree distribution is given by

$$u_{\text{in}}(i,j,k) = \frac{1}{\mu_{100}}(i+1)u(i+1,j,k) \tag{33}$$

Note that the shift of i on the right-hand side refers to the condition that the minimum number of in-edges is one (reached via an in-edge), while i denotes the number of further in-connections. The multiplication factor $(i + 1)$ accounts for the increased probability to reach nodes with more in-edges. Likewise, biased degree distributions for nodes reached by an out- and bidirectional edge are given by

$$\begin{aligned} u_{\text{out}}(i,j,k) &= \frac{1}{\mu_{010}}(j+1)u(i,j+1,k) \\ u_{\text{bi}}(i,j,k) &= \frac{1}{\mu_{001}}(k+1)u(i,j,k+1) \end{aligned} \tag{34}$$

Thus, the generating function of the biased degree distributions can be written as

$$\begin{aligned} U_{\text{in}}(x,y,z) &= \frac{1}{\mu_{100}}\frac{\partial}{\partial x}U(x,y,z) \\ U_{\text{out}}(x,y,z) &= \frac{1}{\mu_{010}}\frac{\partial}{\partial y}U(x,y,z) \\ U_{\text{bi}}(x,y,z) &= \frac{1}{\mu_{001}}\frac{\partial}{\partial z}U(x,y,z) \end{aligned} \tag{35}$$

with $U_{\text{in}}(1, 1, 1) = U_{\text{out}}(1, 1, 1) = U_{\text{bi}}(1, 1, 1) = 1$.

Let us now consider connected components. The size distribution of connected components in the system is denoted as $w(s)$ with its generating function $W(x)$. As the network is tree like, we can define $w_{\text{in}}(s)$ as the size distribution of biased weak components that are reached by following a randomly picked in-edge to its end. In a directed network, the weak component is a component that is built by disregarding the direction of the edges. Analogously, $w_{\text{out}}(s)$ and $w_{\text{bi}}(s)$ are defined as the size distribution of weak components attached to a randomly chosen out- and bidirectional edges. The corresponding generating functions are denoted as $W_{\text{in}}(x)$, $W_{\text{out}}(x)$, and $W_{\text{bi}}(x)$ with $|x| \leqslant 1$ and $x \in \mathbb{C}$ (see **Figure 2** for illustration).

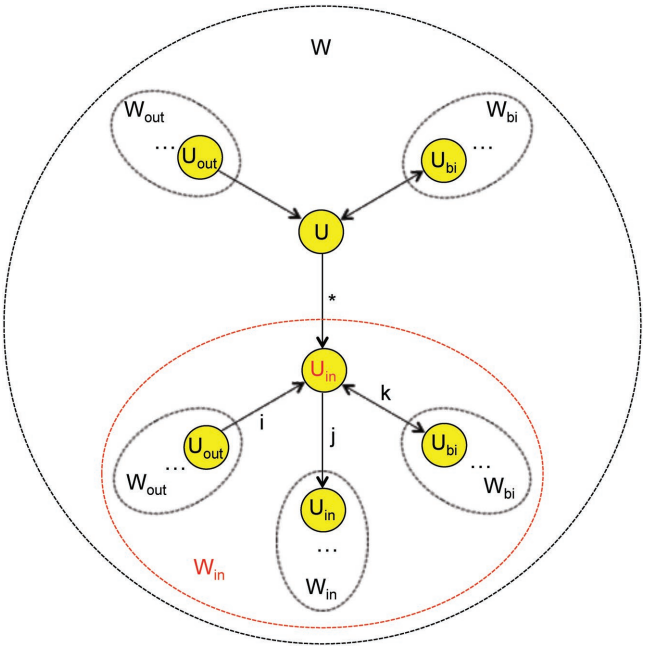

Figure 2. Representation of a random graph in the domain of generating functions for deriving the generating function of the component size distribution $W(x)$. The root node of the component is described by $U(x, y, z)$, the weak component by $W(x)$.

We will now derive an expression for the generating function $W(x)$ departing form $U(x, y, z)$ as the only input for our model.[52] Suppose one selects a node by sampling a random in-edge and following it to its end (edge with "*" in Figure 2). Let the reached node (red "U_{in}" in Figure 2) be the root of a biased weak component with size distribution $w_{\text{in}}(s)$ (red domain in Figure 2). The remaining edges of the root node again lead to roots of biased weak components by i in-, j out-, and k bidirectional edges, with probability $u_{\text{in}}(i, j, k)$. These "second generations" of biased weak components have the same size distributions $w_{\text{in}}(s)$, $w_{\text{out}}(s)$, and $w_{\text{bi}}(s)$. There are i edges connecting the root node to i components $w_{\text{out}}(s)$ (black domain within the red domain in Figure 2, just one of the i domains is shown), j edges to components $w_{\text{in}}(s)$, k edges to components $w_{\text{bi}}(s)$.

Suppose two populations of components are described by two specific size distributions $w_1(s)$ and $w_2(s)$. Consider a process according to which each component from the first population is joined with a randomly selected component from the second population. The size distribution for the resulting population is given by the convolution of the two size distributions, $(w_1*w_2)(s)$. Thus, the distribution of the total size of the i components $w_{\text{out}}(s)$ follows as the i-fold convolution $(w_{\text{out}}*w_{\text{out}}*\cdots*w_{\text{out}})(s)$, which is generated by $W_{\text{out}}(x)^i$. Likewise, the total size distributions of the other two types of weak components are represented by $W_{\text{in}}(x)^j$ and $W_{\text{bi}}(x)^k$. Hence, the size distribution of the biased weak component (red domain) equals the convolution of the three types of biased weak components it is composed of, not yet including the root node. The distribution following from the convolution is given by $\sum_{i,j,k} u_{\text{in}}(i, j, k)W_{\text{out}}(x)^i W_{\text{in}}(x)^j W_{\text{bi}}(x)^k$. The root node is included by

© 2017 The Authors. Published by WILEY-VCH Verlag GmbH & Co. KGaA, Weinheim

increasing the component size by 1, which, in the domain of the generating functions, leads to the factor x in front of the summation

$$W_{\text{in}}(x) = x\sum_{i,j,k} u_{\text{in}}(i,j,k) W_{\text{out}}(x)^i W_{\text{in}}(x)^j W_{\text{bi}}(x)^k \tag{36}$$

Analogously, the relation can be written for $W_{\text{out}}(x)$ and $W_{\text{bi}}(x)$. Equation (36) resembles the definition of a trivariate generating function. Hence, three coupled functional equations are formulated as

$$\begin{aligned} W_{\text{in}}(x) &= xU_{\text{in}}(W_{\text{out}}(x), W_{\text{in}}(x), W_{\text{bi}}(x)) \\ W_{\text{out}}(x) &= xU_{\text{out}}(W_{\text{out}}(x), W_{\text{in}}(x), W_{\text{bi}}(x)) \\ W_{\text{bi}}(x) &= xU_{\text{bi}}(W_{\text{out}}(x), W_{\text{in}}(x), W_{\text{bi}}(x)) \end{aligned} \tag{37}$$

The generating function for the unbiased component size distribution is calculated following the same derivation as for Equation (36), but now realizing that a randomly chosen node is connected to biased components from Equation (37) via three kinds of edges. It is written as

$$W(x) = xU(W_{\text{out}}(x), W_{\text{in}}(x), W_{\text{bi}}(x)) \tag{38}$$

As no analytic expression for $W(x)$ is known, $W(x)$ is obtained by a numerical solution of Equations (37) and (38). The component size distribution $w(s)$, which is the probability of a random node to be part of a component of size s, is obtained by the inverse generating function transform, which is equivalent to the Cauchy integral

$$w(s) = \frac{1}{2\pi i}\oint \frac{W(x)}{x^{s+1}}\,\mathrm{d}x \tag{39}$$

For the numerical evaluation of the integral, the largest possible contour is used, which is given by the unit circle $|x| = 1$ with $x \in \mathbb{C}$.[56]

4.3. Analytic Criterion for the Phase Transition to the Giant Component

In this section, a formula is derived that gives a decisive criterion for the phase transition of the chemical system to the gel regime, corresponding to the phase transition to the giant component in the graph. This criterion requires only the knowledge of the trivariate degree distribution.

The giant component of the network corresponds to an infinite-sized component, the gel in a polymer system. During the polymerization process, polymers grow in size until the gel point is reached. At the gel point, the weight average molecular weight $\langle s\rangle$ becomes singular, as the gel corresponds to a molecule of infinite size. Once the gel is present, the bigger a finite-sized molecule is, the more likely it is to react with the gel. Molecules are "absorbed" by the gel and transit from the sol, the system of finite-sized molecules, to the gel. As the gel is excluded from the definition of the weight average molecular weight $\langle s\rangle$, this process leads to a decrease of $\langle s\rangle$.[58]

The weight average molecular weight $\langle s\rangle$ is given by the first derivative of $W(x)$ evaluated at $x = 1$

$$\begin{aligned} \langle s\rangle &= \frac{W'(x)|_{x=1}}{W(1)} \\ &= \frac{1}{W(1)}\Bigg[1 + \Bigg[W'_{\text{out}}(x)\frac{\partial}{\partial x}U(x,y,z) + W'_{\text{in}}(x)\frac{\partial}{\partial y}U(x,y,z) \\ &\qquad + W'_{\text{bi}}(x)\frac{\partial}{\partial z}U(x,y,z)\Bigg]\Big|_{x,y,z=1}\Bigg] \end{aligned} \tag{40}$$

with $W(1)$ being the normalization factor. Using Equations (37) and (38), calculating the derivatives and inserting into Equation (40) leads to an expression of the form $\langle s\rangle = N/D$. This expression diverges to infinity, if the denominator D approaches zero. After simplification of $D = 0$, the criterion for the phase transition can be written as

$$\begin{aligned} &\mu_{110}^2(2\mu_{001} - \mu_{002}) + \mu_{011}^2(\mu - \mu_{200}) + \mu_{101}^2(\mu - \mu_{020}) \\ &\quad + \mu(\mu_{200} + \mu_{020} - 2\mu_{110})(2\mu_{001} - \mu_{002}) \\ &\quad + 2\mu_{101}\mu_{011}(\mu_{110} - \mu) + \mu_{200}\mu_{020}(\mu_{001} - \mu_{002}) = 0 \end{aligned} \tag{41}$$

with μ_{lmn} denoting the moments of the degree distribution (see Equation (28)) and $\mu_{100} = \mu_{010} = \mu$. In previous works, analytic criteria for the phase transition to a giant component were found for the case of undirected graphs with an univariate degree distribution[59] and the giant weak component for directed graphs with a bivariate degree distribution.[52]

4.4. Gel Fraction

In a polymerization system, the gel fraction g_{f} is defined as the ratio of monomer units in the gel to the total number of monomer units. As the presence of gel in a polymer system corresponds to the existence of a giant component in the graph, the gel fraction g_{f} can also be defined as the ratio of nodes that are part of a giant component to the total number of nodes, which can be interpreted as the relative size of the giant component. The gel point marks the transition point of a graph indicating the first occurrence of a giant component.

The generating function of the component size distribution $W(x)$ does not describe the giant component. Before the gel point, $W(x)$ describes the whole system and satisfies $W(1) = 1$. After the gel point, where $W(x)$ only describes the sol part and $W(1) < 1$, the gel fraction is given by

$$g_{\text{f}} = 1 - W(1) \tag{42}$$

4.5. Crosslinks, FPDBs and Radicals

In this section, distributions and gel fractions for crosslinks, FPDBs, and radicals are derived. The crosslink distribution $w_c(c)$ denotes the probability for a randomly chosen crosslink to be part of a component with c crosslinks. The FPDB distribution $w_v(v)$ gives the probability for a randomly chosen FPDB

© 2017 The Authors. Published by WILEY-VCH Verlag GmbH & Co. KGaA, Weinheim

to be part of a component with v FPDBs. The radical distribution $w_r(r)$ denotes the probability for a randomly chosen radical to be part of a component with r radicals. These distributions correspond to weight distributions. The number distributions are obtained as $\frac{w_c(c)}{c}$, $\frac{w_v(v)}{v}$, and $\frac{w_r(r)}{r}$. The derivations of the crosslink distribution $w_c(c)$, the FPDB distribution $w_v(v)$, and the radical distribution $w_r(r)$ follow the same idea of connected components as the derivation of the component size distribution $w(s)$.

When deriving the crosslink distribution, crosslinks (degree $d = i + j + k > 2$) of a component are counted, whereas nodes that correspond to linear elements ($d = 2$) or dangling ends ($d = 1$) are not counted.

As in the derivation of the size distribution, we start selecting an in-edge and follow it to its end. This time, one may either or not end up in a crosslinking node, as shown by in-edges a and b in **Figure 3**, which circumstance demands to split the problem into two parts. We introduce two degree distributions, one for crosslinking nodes and one for non-crosslinking nodes. The first distribution, which describes crosslinks, is defined as

$$u^{\mathrm{a}}(i,j,k) = \begin{cases} u(i,j,k), & \text{for } d > 2 \\ 0, & \text{for } d \le 2 \end{cases} \tag{43}$$

The second distribution of nodes, accounting for unconnected nodes ($d = 0$), terminal units ($d = 1$) and nodes of $d = 2$, is written as

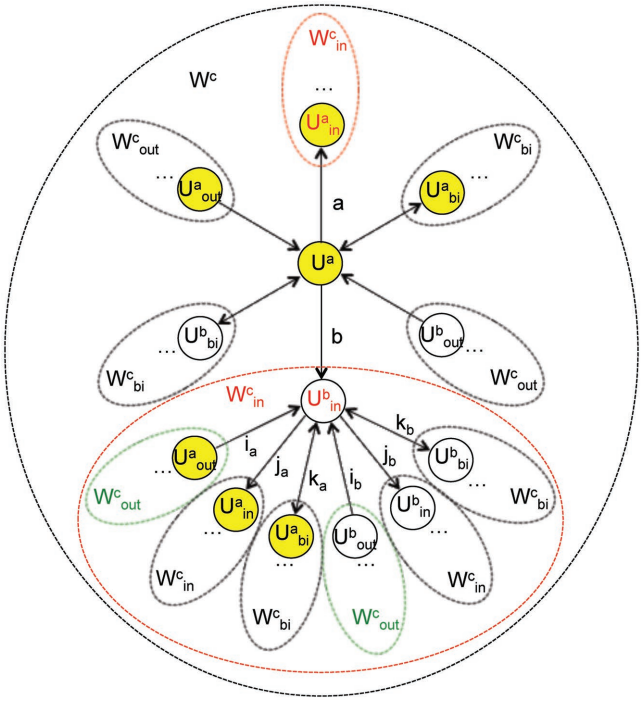

Figure 3. Representation of a random graph in the domain of generating functions for deriving the generating function of the crosslink distribution $W^c(x)$. Only the highlighted nodes are crosslinks and therefore counted.

$$u^{\mathrm{b}}(i,j,k) = \begin{cases} u(i,j,k), & \text{for } d \le 2 \\ 0, & \text{for } d > 2 \end{cases} \tag{44}$$

The corresponding generating functions are defined as

$$\begin{aligned} U^{\mathrm{a}}(x,y,z) &= \sum_{i,j,k} x^i y^j z^k u^{\mathrm{a}}(i,j,k) \\ U^{\mathrm{b}}(x,y,z) &= \sum_{i,j,k} x^i y^j z^k u^{\mathrm{b}}(i,j,k) \end{aligned} \tag{45}$$

with x, y, and z satisfying the same bounds as in Equation (29), and similarly to Equation (35)

$$\begin{aligned} U^{\mathrm{a}}_{\mathrm{in}}(x,y,z) &= \frac{1}{\mu_{100}} \frac{\partial}{\partial x} U^{\mathrm{a}}(x,y,z) \\ U^{\mathrm{b}}_{\mathrm{in}}(x,y,z) &= \frac{1}{\mu_{100}} \frac{\partial}{\partial x} U^{\mathrm{b}}(x,y,z) \end{aligned} \tag{46}$$

Analogously, $U_{\mathrm{out}}(x, y, z)$ and $U_{\mathrm{bi}}(x, y, z)$ are now represented by two functions: one for crosslinks and the other for non-crosslinks.

First, we present the part of the problem involving the crosslinking nodes. It proceeds in exactly the same manner as that for the size distribution before, yielding a convolution term $\sum_{i,j,k} u^{\mathrm{a}}_{\mathrm{in}}(i,j,k) W^c_{\mathrm{out}}(x)^i W^c_{\mathrm{in}}(x)^j W^c_{\mathrm{bi}}(x)^k$, which is the distribution of the biased weak component sizes not yet including the root (a crosslink by definition). In fact, this part of the solution describes the parts of the network exclusively consisting of crosslinking nodes. In Figure 3, this is depicted as the yellow nodes. In-edge "a" connects to a crosslinking node and in-edge "b" to a non-crosslinking node. In the figure, the biased weak components, to which the in-edges "a" and "b" point, are denoted by $W^c_{\mathrm{in}}(x)$ (red domains). However, we only show the content of the component with the non-crosslinking node as the root, characterized by $U^{\mathrm{b}}_{\mathrm{in}}(x,y,z)$. Note that this content is exactly the same as in the other component $W^c_{\mathrm{in}}(x)$, except that the latter has a crosslinking node as the root, characterized by $U^{\mathrm{a}}_{\mathrm{in}}(x,y,z)$. Repeating the procedure for out- and bidirectional edges yields two further convolution terms and ultimately, in the generating function domain, we find these contributions in Equation (47), in the terms with the x in front, due to including the root node.

Next, we derive the part of the distribution associated with the degree distribution of nodes without crosslinks, counting crosslinks connected by non-crosslinking nodes. Root $U^{\mathrm{b}}_{\mathrm{in}}(x,y,z)$ is connected by $i = i_{\mathrm{a}} + i_{\mathrm{b}}$ in-edges to i weak components $W^c_{\mathrm{out}}(x)$ (green domains in Figure 3), again to further nodes, that may either or not be crosslinking nodes. Likewise, there are $j = j_{\mathrm{a}} + j_{\mathrm{b}}$ out- and $k = k_{\mathrm{a}} + k_{\mathrm{b}}$ bidirectional edges connecting to $W^c_{\mathrm{in}}(x)$ and $W^c_{\mathrm{bi}}(x)$, respectively, with the probability distribution $u^{\mathrm{b}}_{in}(i,j,k)$. This leads to the convolution term $\sum_{i,j,k} u^{\mathrm{b}}_{in}(i,j,k) W^c_{\mathrm{out}}(x)^i W^c_{\mathrm{in}}(x)^j W^c_{\mathrm{bi}}(x)^k$, as similar as before, denoting the distribution of the total number of crosslinks in a biased weak component. Since here the root does not contain a crosslink, the total number including the root is equal to this convolution term. This is again repeated for out- and

© 2017 The Authors. Published by WILEY-VCH Verlag GmbH & Co. KGaA, Weinheim

bidirectional edges, which results in further contributions to the generating function Equation (47). Note, that here factor x in front of the summation term is missing, since the root node does not contribute to the number of crosslinks.

Adding the generating function of the crosslink distributions from pure crosslinking parts and from parts counting crosslinks connected by non-crosslinking nodes, we arrive at three coupled functional equations

$$\begin{aligned} W^c_{\text{in}}(x) &= xU^{\text{a}}_{\text{in}}(W^c_{\text{out}}(x), W^c_{\text{in}}(x), W^c_{\text{bi}}(x)) \\ &\quad + U^{\text{b}}_{\text{in}}(W^c_{\text{out}}(x), W^c_{\text{in}}(x), W^c_{\text{bi}}(x)) \\ W^c_{\text{out}}(x) &= xU^{\text{a}}_{\text{out}}(W^c_{\text{out}}(x), W^c_{\text{in}}(x), W^c_{\text{bi}}(x)) \\ &\quad + U^{\text{b}}_{\text{out}}(W^c_{\text{out}}(x), W^c_{\text{in}}(x), W^c_{\text{bi}}(x)) \\ W^c_{\text{bi}}(x) &= xU^{\text{a}}_{\text{bi}}(W^c_{\text{out}}(x), W^c_{\text{in}}(x), W^c_{\text{bi}}(x)) \\ &\quad + U\ \text{b}_{\text{bi}}(W^c_{\text{out}}(x), W^c_{\text{in}}(x), W^c_{\text{bi}}(x)) \end{aligned} \tag{47}$$

They are similar to Equation (37), but they are rewritten in such a way that the number of crosslinks of a component is calculated. To obtain the weight distribution $w_c(c)$, the root node needs to be sampled from the set of crosslinks only. Therefore, the probability of choosing a crosslink as the root is normalized to 1 by $\frac{U^{\text{a}}(x,y,z)}{\mu^{\text{a}}_{000}}$ with

$$\mu^{\text{a}}_{000} = U^{\text{a}}(x,y,z)|_{x=y=z=1} \tag{48}$$

The generating function of the crosslink distribution can be formulated as

$$W^c(x) = \frac{x}{\mu^{\text{a}}_{000}} U^{\text{a}}(W^c_{\text{bi}}(x), W^c_{\text{out}}(x), W^c_{\text{bi}}(x)) \tag{49}$$

To obtain the crosslink distribution $w_c(c)$, the inverse transformation is performed using Equation (39).

The gel fraction for crosslinks is obtained in the same way as the gel fraction of the total material, but now the generating function of the crosslink distribution of Equation (49) is used

$$g^c_{\text{f}} = 1 - W^c(1) \tag{50}$$

It corresponds to the ratio of crosslinks that are part of the gel to the total number of crosslinks. It is important to note that in general Equations (42) and (50) give different gel fractions.

For the derivation of the FPDB distribution, the degree distribution $u(i, j, k)$ is split into two distributions as well: one distribution $u^{\text{a}}(i, j, k)$ of nodes that are counted (with an FPDB) and one distribution $u^{\text{b}}(i, j, k)$ of nodes that are not counted (without an FPDB). As the degree distribution does not include information on FPDBs and radicals, the distributions are extracted from the concentration of the monomer states $g_{\nu,\, r,\, i,\, j,\, k} = [M_{\nu,\, r,\, i,\, j,\, k}]$ (see Equation (23)). The first distribution including nodes with one FPDB is defined as

$$u^{\text{a}}(i,j,k) = \sum_p g_{1,r,i,j,k} \tag{51}$$

the second distribution of nodes without an FPDB is formulated as

$$u^{\text{b}}(i,j,k) = \sum_p (g_{0,r,i,j,k} + g_{2,r,i,j,k}) \tag{52}$$

Thus, $u^{\text{b}}(i, j, k)$ includes nodes without a vinyl group and unconnected nodes with two vinyl groups. Having $u^{\text{a}}(i, j, k)$ and $u^{\text{b}}(i, j, k)$, the same procedure is followed as for crosslinks using Equations (45)–(50). $w_\nu(\nu)$ is obtained by solving Equation (39) with the generating function of the FPDB distribution $W^\nu(x)$ numerically. The gel fraction for FPDBs, the ratio of FPDBs that are part of the gel to the total number of FPDBs, is defined as

$$g^\nu_{\text{f}} = 1 - W^\nu(1) \tag{53}$$

In the case of the radical distribution, three classes of nodes need to be distinguished. The distributions for nodes with one radical, two radicals and without a radical are defined by

$$u^{\text{a1}}(i,j,k) = \sum_\nu g_{\nu,1,i,j,k} \tag{54}$$

$$u^{\text{a2}}(i,j,k) = \sum_\nu g_{\nu,2,i,j,k} \tag{55}$$

and

$$u^{\text{b}}(i,j,k) = \sum_\nu g_{\nu,0,i,j,k} \tag{56}$$

The corresponding generating functions, denoted as $U^{\text{a1}}(x, y, z)$, $U^{\text{a2}}(x, y, z)$, and $U^{\text{b}}(x, y, z)$, as well as the generating functions of the biased distributions are defined analogously to Equations (45) and (46). As nodes with two radicals need to be counted twice, Equation (47) is modified to

$$\begin{aligned} W^r_{\text{in}}(x) &= x^2 U^{\text{a2}}_{\text{in}}(W^r_{\text{out}}(x), W^r_{\text{in}}(x), W^r_{\text{bi}}(x)) \\ &\quad + xU^{\text{a1}}_{\text{bi}}(W^r_{\text{out}}(x), W^r_{\text{in}}(x), W^r_{\text{bi}}(x)) \\ &\quad + U^{\text{b}}_{\text{in}}(W^r_{\text{out}}(x), W^r_{\text{in}}(x), W^r_{\text{bi}}(x)) \\ W^r_{\text{out}}(x) &= x^2 U^{\text{a2}}_{\text{out}}(W^r_{\text{out}}(x), W^r_{\text{in}}(x), W^r_{\text{bi}}(x)) \\ &\quad + xU^{\text{a1}}_{\text{in}}(W^r_{\text{out}}(x), W^r_{\text{in}}(x), W^r_{\text{bi}}(x)) \\ &\quad + U^{\text{b}}_{\text{out}}(W^r_{\text{out}}(x), W^r_{\text{in}}(x), W^r_{\text{bi}}(x)) \\ W^r_{\text{bi}}(x) &= x^2 U^{\text{a2}}_{\text{bi}}(W^r_{\text{out}}(x), W^r_{\text{in}}(x), W^r_{\text{bi}}(x)) \\ &\quad + xU^{\text{a1}}_{\text{bi}}(W^r_{\text{out}}(x), W^r_{\text{in}}(x), W^r_{\text{bi}}(x)) \\ &\quad + U^{\text{b}}_{\text{bi}}(W^r_{\text{out}}(x), W^r_{\text{in}}(x), W^r_{\text{bi}}(x)) \end{aligned} \tag{57}$$

For choosing the root node, a random radical is sampled. The generating function of the radical distribution can be written as

$$\begin{aligned} W^r(x) &= \frac{x^2}{2\mu^{\text{a2}}_{000} + \mu^{\text{a1}}_{000}} 2U^{\text{a2}}(W^r_{\text{out}}(x), W^r_{\text{in}}(x), W^r_{\text{bi}}(x)) \\ &\quad + \frac{x}{2\mu^{\text{a2}}_{000} + \mu^{\text{a1}}_{000}} U^{\text{a1}}(W^r_{\text{out}}(x), W^r_{\text{out}}(x), W^r_{\text{in}}(x)) \end{aligned} \tag{58}$$

with

$$\begin{aligned} \mu^{\text{a2}}_{000} &= U^{\text{a2}}(x,y,z)|_{x=y=z=1} \\ \mu^{\text{a1}}_{000} &= U^{\text{a1}}(x,y,z)|_{x=y=z=1} \end{aligned} \tag{59}$$

The gel fraction of radicals, the ratio of radicals that are part of the gel to the total number of radicals, is calculated by

$$g^r_{\text{f}} = 1 - W^r(1) \tag{60}$$

© 2017 The Authors. Published by WILEY-VCH Verlag GmbH & Co. KGaA, Weinheim

The radical distribution $w_r(r)$ is obtained by the numerical inverse transformation from its generating function $W^r(x)$ using Equation (39).

5. Results

The RGM is demonstrated on the polymerization process of a diacrylate and a photoinitiator under continuous UV irradiation in the absence of oxygen. Kinetic parameters (see Table 1) were obtained from an acrylate modeling study.[9] Since we want to show the ability of the model to predict network properties, we have kept kinetics as simple as possible.

For validation of our RGM, we use the pPBE model for crosslinking polymerization.[48]

5.1. Comparison to the pPBE Model

The polymer model is based on the pPBE defined in Equation (8). The limits of the dimensions are set to $s_{max} = 10^5$ for the component size, $\nu_{max} = 10^5$ for the number of FPDBs per component, and $r_{max} = 8$ for the number of radicals per component. In the pPBE model, a set of Gaussian basis functions is introduced for the approximation of the probability mass function on a logarithmic grid.

For comparison, the concentrations of reacted monomer units, FPDBs, radicals, and crosslinks in sol and gel are calculated with both models. Furthermore, we will compare the gel point prediction in both models.

5.1.1. Concentrations in Pregel and Gel Regime

The total concentration of reacted monomer units c_s, FPDBs c_ν, radicals c_r, crosslinks c_c, initiator $[I_2]$, and initiator radicals $[I]$ are calculated as a function of time. The vinyl conversion χ, the fraction of converted vinyl groups, is defined as

$$\chi = 1 - \frac{c_\nu}{2[M_2](0)} \tag{61}$$

with $[M_2](0)$ denoting the initial concentration of free divinyl monomers (see Table 1). **Figure 4** shows the vinyl conversion χ versus time t and the development of a number of relevant species concentrations as the concentration of crosslinks versus vinyl conversion, ranging from 0% to 100% . The concentrations computed by both models, the RGM and the pPBE model, coincide. As the rate coefficients remain constant over time and trapping of radicals is not implemented explicitly, the final state of the chemical system at $t \to \infty$ is characterized by $c_r \to 0$.

In the pPBE model, the number of crosslinks per molecule is not explicitly included in the reaction mechanism, but is defined by Equation (16) as $c = s - \nu$. This definition accounts for all monomer units without an FPDB. It is important to note that this definition not only includes monomer units that have three or four bonds, but a few units with two bonds as well. These monomer units are formed if one of the vinyl groups undergoes an initiation reaction followed by a termination of the radical. This problem is inherent to the high-molecular formulation of the problem (Equation (8)), since the calculation of the "true" number of crosslinks in that approach requires solving the problem for another dimension—at the expense of more computational time. We did not carry out this extra effort in executing the pPBE approach. Note that the novel random graph approach does not suffer from this problem, as in this approach crosslinks are defined by their degree.

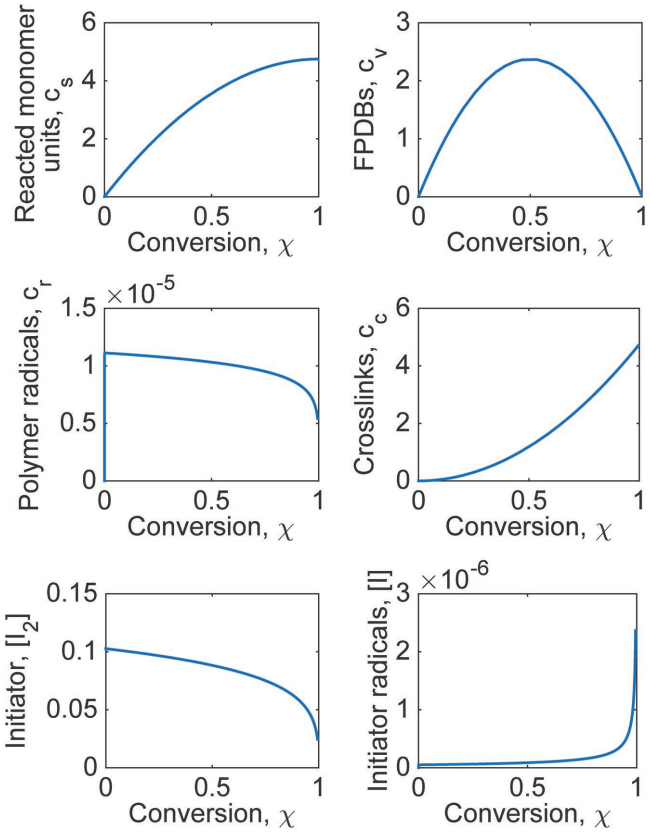

Figure 4. Total concentration (mol L^{-1}) of reacted monomer units c_s, FPDBs c_ν, radicals c_r, crosslinks c_c, initiator $[I_2]$, and initiator radicals $[I]$, as a function of vinyl conversion χ as well as vinyl conversion χ versus time t (s).

Figure 5 zooms in on a vinyl conversion range from 0 to 0.006, which covers the sol–gel transition point that indeed turns out to occur at very low conversion. In this figure, additionally to the concentrations of the total system (blue line), the concentrations in the sol are illustrated, predicted by the RGM (red line) and pPBE (green line) models. In the RGM, the values are obtained by first calculating the gel fractions g_f, g_f^c, g_f^ν and g_f^r (see Sections 4.4 and 4.5). The gel fraction in Equation (42), g_f, is defined as the fraction of monomer units in gel to the total amount of monomer units. Since it is relevant to relate the gel fraction to reacted monomers only, we introduce

$$g_f^{pol} = g_f \frac{[M_2](0)}{c_s} \tag{62}$$

© 2017 The Authors. Published by WILEY-VCH Verlag GmbH & Co. KGaA, Weinheim

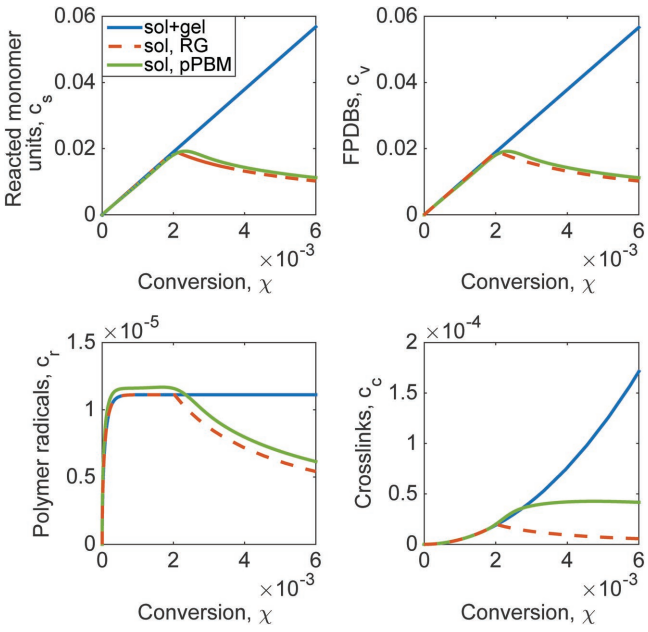

Figure 5. Concentrations (mol L^{-1}) of reacted monomer units, FPDBs, radicals, and crosslinks as a function of conversion χ in the total system (c_s, c_v, c_r, c_c), and the sol ($c_{s,\,\mathrm{sol}}$, $c_{v,\,\mathrm{sol}}$, $c_{r,\,\mathrm{sol}}$, $c_{c,\,\mathrm{sol}}$) predicted by the RGM and the pPBE model.

The concentrations in the sol of different species are then calculated by

$$\begin{aligned} c_{s,\mathrm{sol}} &= c_s(1-g_f^{\mathrm{pol}}) \\ c_{c,\mathrm{sol}} &= c_c(1-g_f^{c}) \\ c_{v,\mathrm{sol}} &= c_v(1-g_f^{v}) \\ c_{r,\mathrm{sol}} &= c_r(1-g_f^{r}) \end{aligned} \tag{63}$$

Naturally, before the gel point, the concentrations in sol equals the total concentrations $c_{i,\mathrm{sol}} = c_i$. After a conversion of 0.002, the gel point conversion χ_{gel}, the concentrations change significantly, which indicates the formation and growth of the gel.

The green line corresponds to the result of the pPBE model. The concentrations in the sol are directly given by the first moments of $f_{s,\,v,\,r}$ (see Equation (15)).

Ideally, both models (red and green lines) should produce the same results. Considering the reacted monomer units and the FPDBs, good agreement is observed for the whole range of conversion. However, some discrepancy is observed, in particular at the gel point. It should be noted that at the gel point all the distributions possess long tails, as explained in Section 5.2. This requires the pPBE model to yield solutions until very high numbers of monomer units, FPDBs, etc. A trade-off between accuracy and computational time forces to impose cut-off lengths at the tails of the distributions. This is the main cause of the deviations between the pPBE and the RGM model. For instance, at the gel point the discontinuity is not predicted as sharply in the pPBE model as in the RGM.

Also, the crosslink distributions diverge at low conversion. Note that the pPBE does not explicitly give the crosslink distribution, but it follows as the difference between monomer units and FPDBs. Obviously, since both distributions have numerical errors even larger deviations are expected in the differential (crosslink) distribution.

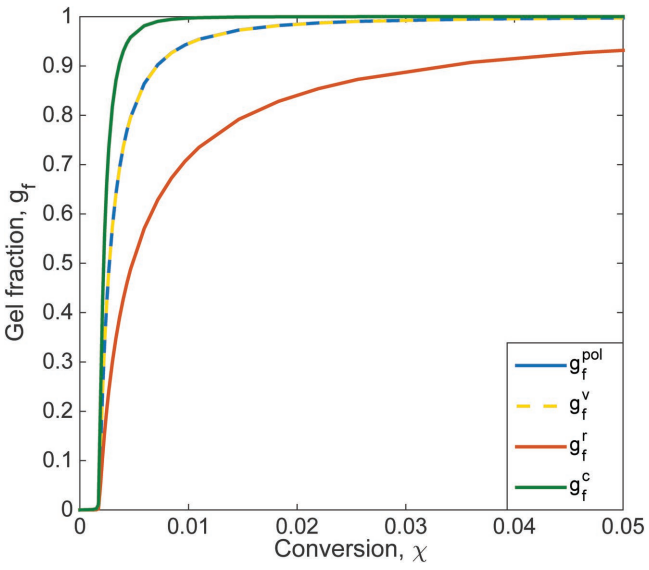

Figure 6. Gel fractions of reacted monomers g_f^{pol}, FPDBs g_f^{v}, radicals g_f^{r}, and crosslinks g_f^{c} as a function of conversion χ.

In **Figure 6**, the different gel fractions calculated by the RGM are illustrated for a conversion range from 0 to 0.05. Here, one observes the remarkable fact that all polymers are already part of the network at conversions as low as 2%. The gel fraction of FPDBs g_f^{v} coincides with the gel fraction of reacted monomers g_f^{pol}. Note that this is not the case for the gel fractions of radicals g_f^{r} and crosslinks g_f^{c}. The probability for radicals of being part of the gel g_f^{r} is lower than for the overall material g_f^{pol}, whereas the probability for crosslinks of being part of the gel g_f^{c} is higher than g_f^{pol}. This behavior is caused by the different processes these species are formed. Radicals are produced by the initiation of vinyl groups. As at a low conversion the highest concentration of vinyl groups lies in the group of unreacted monomers, initiation causes these monomer units to transit to the sol and therefore increases the relative concentration of radicals in the sol. On the other hand, crosslinks are only formed by reacting a monomer unit that is already part of a polymer molecule, so its probability to transit to gel, or of already being part of the gel, is considerably higher than of being part of the sol.

5.1.2. Gel Point Estimation

In the previous section, the gel point became clearly visible as the conversion point at which the gel fraction starts to depart from zero. However, the analytic criterion for the existence of the giant component derived in Section 4.3 provides a way to find the gel point directly from the time-dependent trivariate degree distribution defined in Equation (26). The gel point conversion χ_{gel} is estimated by calculating the moments of the

© 2017 The Authors. Published by WILEY-VCH Verlag GmbH & Co. KGaA, Weinheim

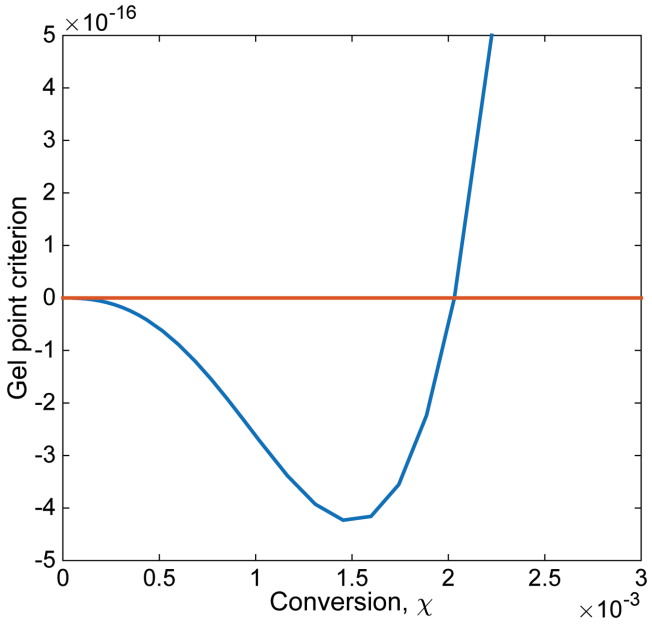

Figure 7. Gel point estimation by the RGM by the evaluation of the analytic gel point criterion as a function of conversion χ. The crossing of the lines indicates the gel point at a conversion of $\chi_{gel} = 0.0020$.

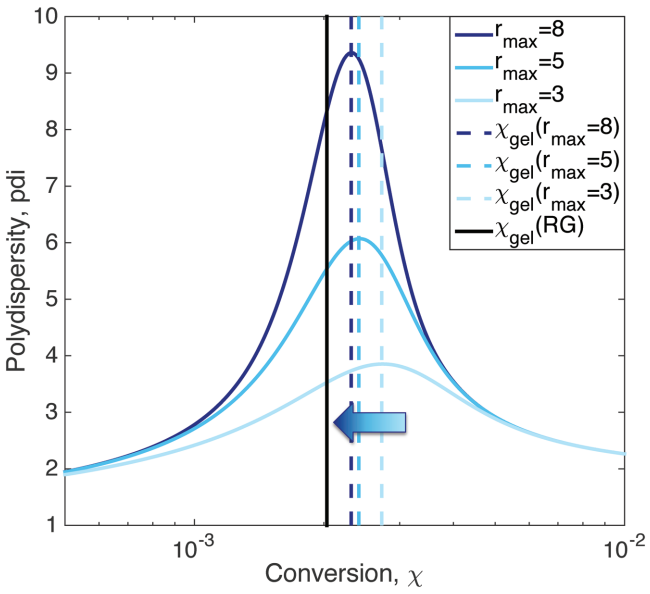

Figure 8. Gel point estimation by the pPBE. The solid blue lines illustrate the polydispersity for different r_{max}. The dashed lines indicate the maximum of the pdi, which corresponds to the gel point estimate. For higher r_{max}, a shift of the maximum to lower conversion is observed. The black line indicates the gel point estimation from the RGM.

degree distribution and inserting them into Equation (41). The main advantage of the criterion is that it avoids the numerical solution of Equations (37) and (38). This means, that numerical errors are reduced to a minimum and the computation is very fast.

For the problem of the photocuring of the diacrylate system, the gel point is estimated at a vinyl conversion of $\chi_{gel} = 0.0020$. The result of the numerical evaluation of the criterion is illustrated in **Figure 7**.

For the pPBE model, the gel point is estimated by calculating the polydispersity

$$pdi = \frac{m_2 m_0}{m_1^2} \tag{64}$$

with

$$\begin{aligned} m_2 &= \sum_{s,\nu,r} s^2 f_{s,\nu,r} \\ m_1 &= \sum_{s,\nu,r} s f_{s,\nu,r} \\ m_0 &= \sum_{s,\nu,r} f_{s,\nu,r} \end{aligned} \tag{65}$$

denoting the second, first, and zeroth moments of the molecular number distribution. The polydispersity is singular at the gel point. The gel point conversion χ_{gel} is defined as the conversion, where the polydispersity reaches its maximum. **Figure 8** shows a dependency of the gel point estimation on the maximal number of radicals per component r_{max}. The higher the r_{max}, the sharper the observed peak becomes, and a shift to lower conversion is observed: $\chi_{gel}(r_{max} = 8) = 0.0023$, $\chi_{gel}(r_{max} = 5) = 0.0024$, $\chi_{gel}(r_{max} = 3) = 0.0027$.

5.2. Distributions

In Sections 4.2 and 4.5, methods for calculating the component size, crosslink, FPDB, and radical distributions are developed.

In **Figure 9**, the double-weighted distribution of molecular sizes $[M_2](0)M_x sw(s, \chi)$ (molar mass of diacrylate M_x, see Table 1 for numerical values) is depicted for several conversion points before and after the gel point. One may notice the shift of the peaks in the plot. The distribution at gel conversion χ_{gel} is observed to be very broad and goes far beyond the cut-off size of 10^4. The asymptotic behavior at the gel conversion is discussed in more detail for the single-weighted distribution $[M_2](0)w(s, \chi)$.

In **Figure 10**, the component size distribution normalized to the sol concentration $[M_2](0)w(s, \chi)$ is given for different conversion points χ. As unreacted monomer units are not included in the graphic, the distribution starts at a low concentration for components of size $s = 2$ and shows an exponential decrease for larger components. For higher conversion, the distributions gradually become broader as components grow in size. However, the distributions still show exponential decrease. Concerning the asymptotic behavior of the size distribution curves at phase transitions like the gel point, theories have been constructed based on universal characteristic of polymerization and aggregation problems. It has been shown for a very broad range of aggregation models that the tail of the size distribution obeys a power law $w(s, \chi_{gel}) \propto s^{-\tau}$ with τ being the Fisher exponent. When no information on spatial configuration is taken into account, at the gel point the Fisher exponent is expected to have a value of $\tau = \frac{3}{2}$ for the weighted distribution of the component size $w(s, \chi_{gel})$.[58] The dashed black line in Figure 10

© 2017 The Authors. Published by WILEY-VCH Verlag GmbH & Co. KGaA, Weinheim

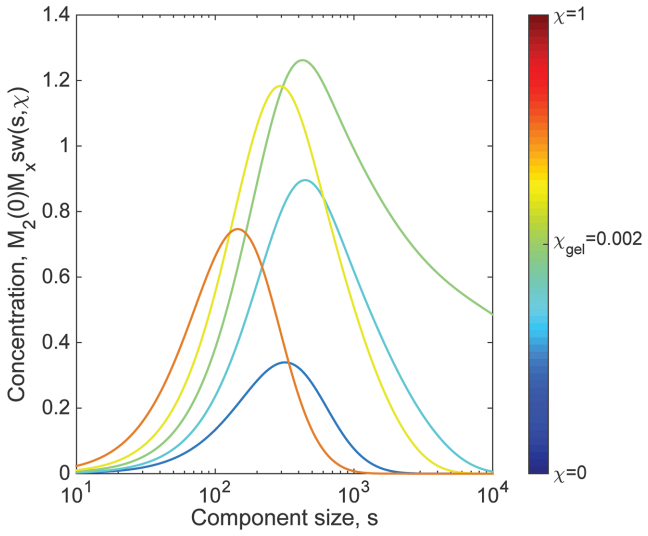

Figure 9. Double-weighted distribution of molecules of size s normalized to the concentration in sol for different conversion χ (indicated by the color).

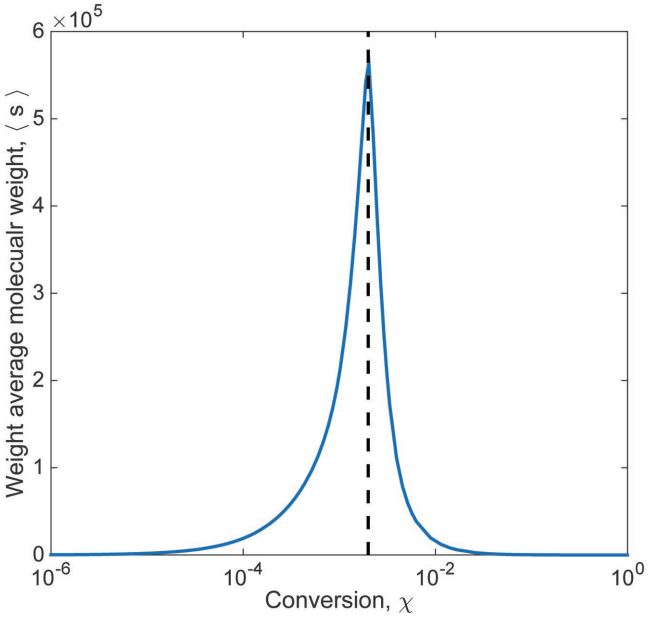

Figure 11. Weight average molecular weight $\langle s \rangle$ as a function of conversion χ. The peak coincides with the gel point estimation from the gel point criterion (black dashed line).

corresponds to the theoretical asymptotic behavior of the tail of the component size distribution, the Fisher exponent.

The algebraic decrease of the tail at the gel point causes the singularity of the weight average molecular weight $\langle s \rangle$ at χ_{gel}, shown in **Figure 11**. In **Figure 12**, the component size distribution is shown as a function of conversion and component size.

Far from the gel point assigning low values to the cut-off value for the number of radicals in the pPBE model still leads to good results. However, close to the gel point, polymers with a large number of radicals are formed and gain importance. At the gel point, the radical distribution obeys the same power law as the component size distribution. This is typically a problem for the pPBE model, as it relies on the limitations of its dimensions. In contrast, the RGM does not suffer from this problem. **Figure 13** illustrates the concentration of polymers in sol with $r \in 1, \ldots, 500$ radicals as a function of conversion χ computed by the RGM. The concentration is calculated by the number distribution of radicals normalized to the concentration of radicals in sol, $\frac{w_r(r,\chi)}{r} c_r(\chi)$. This figure proves that in conversion regions at some distance from the gel point concentrations of molecules with many radicals are negligible. However, it also demonstrates that near the gel point multiradical molecules are formed with numbers of radicals of several hundreds.

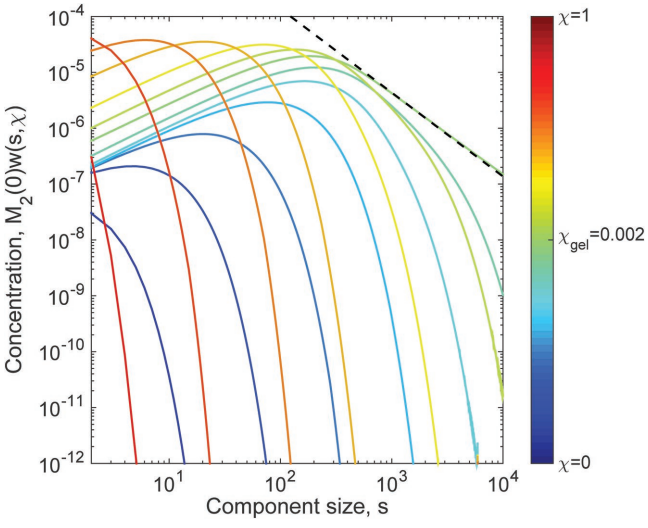

Figure 10. Concentration (mol L^{-1}) of monomer units/nodes that are part of a molecule/component of size s in sol for different conversion χ (indicated by the color). The dashed black line visualizes the asymptotic behavior $w(s, \chi_{gel}) \propto s^{-\tau}$ with the Fisher exponent $\tau = \frac{3}{2}$.

Figure 14 illustrates the weighted crosslink distribution normalized to the concentration in sol $c_c(\chi)w_c(c, \chi)$ with its generating function being defined by Equation (49). It defines the concentration of crosslinks that are part of a connected component with c crosslinks at conversion χ. Note that the concentration of crosslinks was already shown in Figure 5. At the gel point, it is still relatively low, 2×10^{-5} mol L^{-1}. Realizing that the concentration of monomer units in polymer at the gel point is 0.02 mol L^{-1}, the average crosslink density is given by 1×10^{-3}. One may estimate the average length of linear polymer segments (chains without crosslinks, lengths between crosslinks, free dangling ends) to be 1000 monomer units. Hence, the network close beyond the gel point is very sparse. Even, at 2% conversion, when practically all polymer (98%) belongs to gel, the crosslink density is still low, and the average linear segment amounts to ≈100 units. Note that both the crosslink density and its distribution as shown in Figure 14 are important characteristics of the polymer network, directly linked to material properties like elasticity.[33,60] Hence, information concerning crosslinks forms an important means of validation of our model.

© 2017 The Authors. Published by WILEY-VCH Verlag GmbH & Co. KGaA, Weinheim

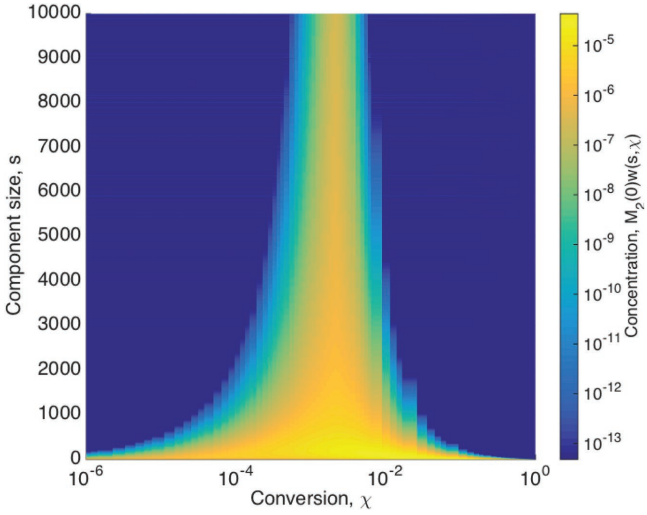

Figure 12. Concentration (mol L^{-1}, indicated by color) of monomer units/nodes in sol that are part of a molecule/component of size s as a function of conversion χ.

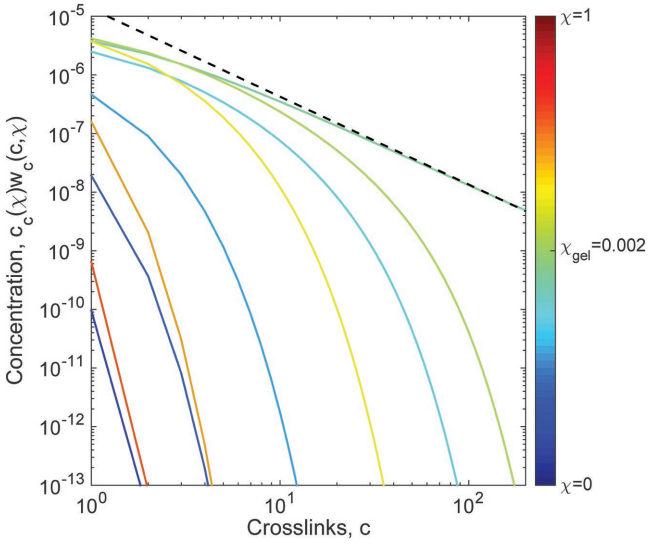

Figure 14. Concentration (mol L^{-1}) of crosslinks in sol that are part of a molecule with c crosslinks for different conversion χ (indicated by the color). The dashed black line indicates the asymptotic behavior $w_c(c, \chi_{gel}) \propto c^{-\tau}$ with $\tau = \frac{3}{2}$.

6. Conclusion

A random graph model was developed to predict the topology of an evolving polymer network formed by free-radical photopolymerization. The formation of the network is considered as a random process, but governed by a well-formulated reaction mechanism. The polymer network is viewed as a random graph with directed and undirected edges. The random graph is completely defined by a time-dependent trivariate degree distribution. The degree distribution, which acts as the input of the random graph, is obtained by the numerical solution of the mPBE defining the concentration of monomer states.

The system includes all the relevant photocuring reactions, but excludes inhibition reactions. As another simplifying assumption, the decrease of rate coefficients due to diffusion limitations has not been accounted for.

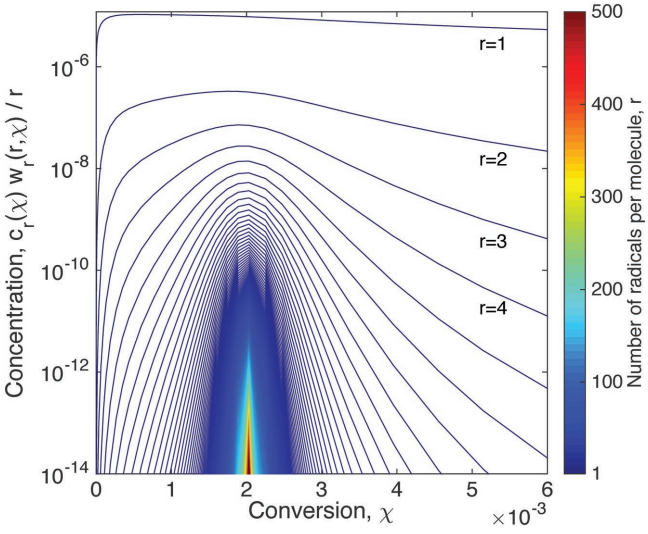

Figure 13. Concentration (mol L^{-1}) of polymers with $r \in 1, \ldots, 500$ radicals as a function of conversion χ. The number of radicals is indicated by the color.

In comparison to the pPBE, formulated for the same system, the number of differential equations that need to be solved is much lower. The solution of the mPBE provides information on the number and type of bonds for all monomer units for the whole range of conversion. Therefore, local information on the topology of the network is available also for the gel regime.

Global properties of the network are predicted over the whole range of photocuring conditions from low-viscosity monomer to the fully solid polymer network using the random graph formalism. The concentrations of reacted monomer units, FPDB, radicals, and crosslinks in sol and gel are estimated by computing the corresponding gel fractions. The results are compared to the solution of a "classical" pPBE.[48] For the reacted monomer units, FPDBs, and radicals, the results of the two models are in good agreement. As the pPBE model is formulated for a 3D distribution (size, FPDBs, and radicals), the number of crosslinks is not explicitly accounted for. Numerical errors in the pPBE prevent a reliable estimation of concentration of crosslinks in the sol after the gel point. In contrast, the concentration of crosslinks is directly accessible in the RGM. Additionally, the RGM is easily extendable to high dimensions to include additional properties of monomers. An extension only requires the adjustment of the formulation of the mPBE, the RGM remains the same.

An important property of evolving networks is the emergence of the gel. An analytic criterion is presented, which allows the determination of the exact the gel point. This criterion utilizes only moments of the temporal degree distribution as input. In the pPBE model, an exact gel point estimation is not possible due to the limits on the sizes of its dimension. Especially polymers with high numbers of radicals become important in the region close to the gel point, which can only be considered in the RGM.

© 2017 The Authors. Published by WILEY-VCH Verlag GmbH & Co. KGaA, Weinheim

The RGM provides the possibility of computing the weight distributions of component size, FPDBs, radicals, and crosslinks. The cut-off of the distributions is not an intrinsic property of the model, but can be chosen freely.

Under the model assumptions the gel point is predicted at a remarkably low vinyl conversion of 0.2%, while at 2% conversion almost all polymer present (98%) already belongs to the gel (based on counting monomer units). From the concentration of crosslinks we may estimate the average length of the linear strands: linear chains, chain segments between crosslinks, and dangling segments. At the gel point, these strands in average count 1000 monomer units. Thus, our model reveals the interesting nature of the polymer material at low-conversion stages of 2% as being one relatively sparse network molecule. This picture may change when applying decreasing reaction rates, for instance, by a quantitative feedback from the evolving network topology leading to lower mobility of reacting functional groups. Moreover, allowing for cycles of arbitrary size in the sol part of the system might change the observed topology fundamentally.

Tracking the mobility of the reactive groups during the phase transition and in the early gel stages and the quantification of the consequences for the reaction rates as well as the implementation of cycles already at early conversion will be objectives of our further modeling studies. Further validation will be explored through measurement of mechanical properties of experimental acrylate networks.

Abbreviations

FPDB	free pending double bond
MC	Monte Carlo
mPBE	monomer PBE
PBE	population balance equation
pPBE	polymer PBE
RGM	random graph model

Nomenclature

$(g^*f)(x)$	Convolution of the functions $g(x)$ and $f(x)$
$[I_2](0)$	Initial concentration of photoinitiator
$[M_2](0)$	Initial concentration of diacrylate
$[X]$	Molar concentration of X
χ	Vinyl conversion
χ_{gel}	Vinyl conversion at the gel point
$\dot{X}$	Time derivative of X
μ_{lmn}	Partial moments of the degree distribution
τ	Fisher exponent
Θ	Heaviside function
c	Number of crosslinks
c_c	Molar concentration of crosslinks
c_r	Molar concentration of radicals
c_s	Molar concentration of reacted monomer units
c_ν	Molar concentration of FPDBs
c'_ν	Molar concentration of vinyl groups
$c_{c,\,sol}$	Molar concentration of crosslinks in sol
$c_{r,\,sol}$	Molar concentration of radicals in sol
$c_{s,\,sol}$	Molar concentration of reacted monomer units in sol
$c_{\nu',sol}$	Molar concentration of vinyl groups in sol
$c_{\nu,\,sol}$	Molar concentration of FPDBs in sol
d	Node degree
$f_{s,\,\nu,\,r}$	Molar concentration of polymer molecules with state $\{s, r, \nu\}$
g_f	Gel fraction of momomer units
g_f^{pol}	Gel fraction of reacted momomer units
g_f^c	Gel fraction of crosslinks
g_f^r	Gel fraction of radicals
g_f^ν	Gel fraction of FPDBs
$g_{\nu,\,r,\,i,\,j,\,k}$	Molar concentration of monomer units with state $\{\nu, r, i, j, k\}$
I	Initiator radical
i	Number of in-bonds/edges
I_2	Photoinitiator
j	Number of out-bonds/edges
k	Number of bidirectional bonds/edges
k_d	Rate coefficient for photoinitiation
k_i	Rate coefficient for vinyl initiation
k_p	Rate coefficient for propagation
k_{tc}	Rate coefficient for termination by recombination
k_{td}	Rate coefficient for termination by disproportionation
m_0	0^{th} moment of the molecular number distribution in sol
m_1	1^{st} moment of the molecular number distribution in sol
M_2	Free divinyl monomer
m_2	2^{nd} moment of the molecular number distribution in sol
M_x	Molar mass of the diacrylate
$M_{\nu,\,r,\,i,\,j,\,k}$	Monomer unit with ν vinyl groups, r radicals, i in-bonds, j out-bonds and k bidirectional bonds
$P_{s,\,\nu,\,r}$	Polymer molecule with size s, ν vinyl groups and r radicals
pdi	Polydispersity
r	Number of radicals
s	Size of the polymer molecule
t	Time
$u(i, j, k)$	Degree distribution
$U(x, y, z)$	Generating function of the degree distribution
$u_{bi}(i, j, k)$	Degree distribution for nodes reached by a bidirectional edge
$U_{bi}(x, y, z)$	Generating function of $u_{bi}(i, j, k)$
$u_{in}(i, j, k)$	Degree distribution for nodes reached by an in-edge
$U_{in}(x, y, z)$	Generating function of $u_{in}(i, j, k)$
$u_{out}(i, j, k)$	Degree distribution for nodes reached by an out-edge
$U_{out}(x, y, z)$	Generating function of $u_{out}(i, j, k)$
ν	Number of vinyl groups
$w(s)$	Size distribution of a weak component
$W(x)$	Generating function of $w(s)$
$W_{bi}(s)$	Generating function of $w_{bi}(s)$
$w_{bi}(s)$	Size distribution of a weak component reached by a bidirectional edge
$W_{in}(s)$	Generating function of $w_{in}(s)$
$w_{in}(s)$	Size distribution of a weak component reached by an in-edge

© 2017 The Authors. Published by WILEY-VCH Verlag GmbH & Co. KGaA, Weinheim

$W_{out}(s)$	Generating function of $w_{out}(s)$
$w_{out}(s)$	Size distribution of a weak component reached by an out-edge
$w_c(c)$	Crosslink distribution
$w_r(r)$	Radical distribution
$w_v(v)$	Vinyl distribution
x	Indeterminate of the generating function
y	Indeterminate of the generating function
z	Indeterminate of the generating function

Supporting Information

Supporting Information is available from the Wiley Online Library or from the author.

Acknowledgements

This research was supported by Océ Technologies B.V. and the Technology Foundation STW. I.K. acknowledges support form research program Veni with project number 639.071.511, which is financed by the Netherlands Organisation for Scientific Research (NWO).

Conflict of Interest

The authors declare no conflict of interest.

Keywords

acrylate network, gel transition, radical polymerization, random graph, reaction kinetics

Received: June 12, 2017
Revised: August 8, 2017
Published online: September 18, 2017

[1] V. Litvinov, A. Dias, *Macromolecules* **2001**, *34*, 4051.
[2] D. L. Safranski, K. Gall, *Polymer* **2008**, *49*, 4446.
[3] M. Wen, L. Scriven, A. V. McCormick, *Macromolecules* **2003**, *36*, 4151.
[4] A. Boddapati, S. B. Rahane, R. P. Slopek, V. Breedveld, C. L. Henderson, M. A. Grover, *Polymer* **2011**, *52*, 866.
[5] P. J. Flory, *J. Am. Chem. Soc.* **1941**, *63*, 3083, https://doi.org/10.1021/ja01856a061.
[6] J. M. Asua, S. Beuermann, M. Buback, P. Castignolles, B. Charleux, R. G. Gilbert, R. A. Hutchinson, J. R. Leiza, A. N. Nikitin, J.-P. Vairon, A. M. van Herk, *Macromol. Chem. Phys.* **2004**, *205*, 2151.
[7] C. Barner-Kowollik, S. Beuermann, M. Buback, P. Castignolles, B. Charleux, M. L. Coote, R. A. Hutchinson, T. Junkers, I. Lacik, G. T. Russell, M. Stach, A. M. van Herk, *Polym. Chem.* **2014**, *5*, 204.
[8] W. Wang, R. A. Hutchinson, *AIChE J.* **2011**, *57*, 227.
[9] M. D. Goodner, C. N. Bowman, *Chem. Eng. Sci.* **2002**, *57*, 887.
[10] A. K. O'Brien, C. N. Bowman, *Macromolecules* **2006**, *39*, 2501.
[11] A. K. O'Brien, C. N. Bowman, *Macromol. Theory Simul.* **2006**, *15*, 176.
[12] C. N. Bowman, C. J. Kloxin, *AIChE J.* **2008**, *54*, 2775.
[13] P. M. Johnson, J. W. Stansbury, C. N. Bowman, *Macromolecules* **2008**, *41*, 230.
[14] A. K. O'Brien, C. N. Bowman, *Macromolecules* **2003**, *36*, 7777.
[15] T. M. Lovestead, J. A. Burdick, K. S. Anseth, C. N. Bowman, *Polymer* **2005**, *46*, 6226.
[16] G. A. Miller, L. Gou, V. Narayanan, A. B. Scranton, *J. Polym. Sci., Part A: Polym. Chem.* **2002**, *40*, 793.
[17] J. Lange, N. Davidenko, J. Rieumont, R. Sastre, *Macromol. Theory Simul.* **2004**, *13*, 641.
[18] S. Zhu, Y. Tian, A. Hamielec, D. Eaton, *Macromolecules* **1990**, *23*, 1144.
[19] K. S. Anseth, K. J. Anderson, C. N. Bowman, *Macromol. Chem. Phys.* **1996**, *197*, 833.
[20] K. S. Anseth, C. M. Wang, C. N. Bowman, *Macromolecules* **1994**, *27*, 650.
[21] K. S. Anseth, C. N. Bowman, *Polym. React. Eng.* **1993**, *1*, 499.
[22] C. W. Macosko, D. R. Miller, *Macromolecules* **1976**, *9*, 199.
[23] D. R. Miller, C. W. Macosko, *Rubber Chem. Technol.* **1976**, *49*, 1219.
[24] T. M. Lovestead, C. N. Bowman, *Macromolecules* **2005**, *38*, 4913.
[25] S. K. Reddy, O. Okay, C. N. Bowman, *Macromolecules* **2006**, *39*, 8832.
[26] K. Dušek, *Polym. Bull.* **1985**, *13*, 321.
[27] K. Dušek, *Developments in Polymerization, 3. Network Formation and Cyclization in Polymer Reactions*, Applied Science Publishers, London, UK **1982**.
[28] J. Mikes, K. Dušek, *Macromolecules* **1982**, *15*, 93.
[29] W. H. Stockmayer, *J. Chem. Phys.* **1943**, *11*, 45, https://doi.org/10.1063/1.1723803.
[30] R. M. Ziff, *J. Stat. Phys.* **1980**, *23*, 241.
[31] A. B. Scranton, N. A. Peppas, *J. Polym. Sci., Part A: Polym. Chem.* **1990**, *28*, 39.
[32] H. Galina, A. Szustalewicz, *Macromolecules* **1989**, *22*, 3124.
[33] K. Dušek, M. Dušková-Smrčková, *Prog. Polym. Sci.* **2000**, *25*, 1215.
[34] J. Šomvársky, K. Dušek, M. Smrčková, *Comput. Theor. Polym. Sci.* **1998**, *8*, 201.
[35] H. Tobita, *Macromol. Theory Simul.* **2015**, *24*, 117.
[36] I. Kryven, P. D. Iedema, *Chem. Eng. Sci.* **2015**, *126*, 296.
[37] I. Kryven, P. D. Iedema, *Macromol. React. Eng.* **2015**, *9*, 285.
[38] I. Kryven, P. D. Iedema, *Macromol. Theory Simul.* **2014**, *23*, 7.
[39] P. Pladis, C. Kiparissides, *Chem. Eng. Sci.* **1998**, *53*, 3315.
[40] A. Brandolin, A. A. Balbueno, M. Asteasuain, *Comput. Chem. Eng.* **2016**, *94*, 272.
[41] I. Zapata-González, R. A. Hutchinson, K. A. Payne, E. Saldívar-Guerra, *AIChE J.* **2016**, *62*, 2762.
[42] H. Galina, J. Lechowicz, *Polymer* **2000**, *41*, 615.
[43] E. R. Duering, K. Kremer, G. S. Grest, *J. Chem. Phys.* **1994**, *101*, 8169.
[44] S. Hamzehlou, Y. Reyes, J. R. Leiza, *Macromolecules* **2013**, *46*, 9064.
[45] G. Arzamendi, J. R. Leiza, *Ind. Eng. Chem. Res.* **2008**, *47*, 5934.
[46] Z. Zhou, D. Yan, *Polymer* **2006**, *47*, 1473.
[47] M. Asteasuain, C. Sarmoria, A. Brandolin, *Polymer* **2002**, *43*, 2513.
[48] I. Kryven, P. Iedema, *Polymer* **2014**, *55*, 3475.
[49] I. Kryven, S. Röblitz, C. Schütte, *BMC Syst. Biol.* **2015**, *9*, 67.
[50] B. Eichinger, *Polymer* **2005**, *46*, 4258.
[51] E. Ben-Naim, P. Krapivsky, *Phys. Rev. E* **2005**, *71*, 026129.
[52] I. Kryven, *Phys. Rev. E* **2016**, *94*, 012315.
[53] I. Kryven, J. Duivenvoorden, J. Hermans, P. D. Iedema, *Macromol. Theory Simul.* **2016**, *25*, 449.
[54] I. Kryven, *Phys. Rev. E* **2017**, *95*, 052303.
[55] K. Dušek, M. Dušková-Smrčková, *Macromol. React. Eng.* **2012**, *6*, 426.
[56] M. E. J. Newman, S. H. Strogatz, D. J. Watts, *Phys. Rev. E* **2001**, *64*, 026118.
[57] S. Zhu, A. E. Hamielec, *Macromolecules* **1993**, *26*, 3131.
[58] M. Rubinstein, R. Colby, *Polymer Physics*, OUP, Oxford, UK **2003**.
[59] M. Molloy, B. Reed, *Random Struct. Algor.* **1995**, *6*, 161.
[60] A. Zlatanić, Z. S. Petrović, K. Dušek, *Biomacromolecules* **2002**, *3*, 1048.

© 2017 The Authors. Published by WILEY-VCH Verlag GmbH & Co. KGaA, Weinheim